

A Macro Projective Integration Method in 2D Microscopic System Applied to Nonlinear Ion Acoustic Waves in a Plasma

A. M. Maluckov^{1,2}, S. Ishiguro^{1,*} and M. M. Škorić¹

¹ National Institute for Fusion Science, Toki, 509-5292, Japan.

² Faculty of Science, University of Niš, 18001, Serbia.

Received 19 November 2007; Accepted (in revised version) 20 December 2007

Available online 14 April 2008

Abstract. In the *Equation-free* framework, a macro-coarse projective integration method consists of two parts: the time stepper and time projection on macro scale. The first one consists of lifting, micro simulation and restriction. For extracting directly from microscopic simulations the information which would be obtained from the macroscopic model of two-dimensional microscopic systems, the time stepper based on the one-dimensional cumulative distribution functions, the marginal cumulative and appropriate number of the conditional cumulative distributions, is introduced. Here this procedure is tested on the nonlinear ion acoustic wave in a plasma. The numerical micro-solver is the one dimensional electrostatic particle-in-cell code. It is shown that particle correlations related to wave structures are better preserved by the new model. The lifting step is critically related to the noise in system. The enlarged noise, rise of correlations, trapping of particles during the wave steepening can seriously violate the basic assumptions of the equation-free approach.

AMS subject classifications: 68U20, 81T80

Key words: Multiscale simulations, E-free framework, nonlinear plasmas.

1 Introduction

The macroscopic, e.g., coherent behavior in the complex systems emerges in the interactions of microscopic constituents-atoms, molecules, cells, individuals of a population-among themselves and with an environment. As a consequence the macroscopic behavior can somehow be deduced from the microscopic one. For some problems like

*Corresponding author. *Email addresses:* sandra@pmf.ni.ac.yu (A. M. Maluckov), ishiguro.seiji@nifs.ac.jp (S. Ishiguro), skoric.milos@nifs.ac.jp (M. M. Škorić)

Newtonian fluid mechanics the Navier-Stokes equation predated its microscopic derivation from the kinetic theory. However, in many problems in chemistry, ecology, material science, engineering, etc. the closures required to translate them from the microscopic (particle) level to a high-level macroscopic description are unknown. Severe limitations arise in trying either to find closures or to solve these problems at the scale at which the questions of interest are asked, by using microscopic simulations only. The *Equation-free* (EFREE) proposed by I.G. Kevrekidis et al. [1–4] is one of the systematic frameworks for directly extracting from microscopic simulations the information which would be obtained from macroscopic models had these been available in a closed form. This is a system based procedure processing the results of short bursts of appropriately initialized microscopic simulations.

The main tool that allows the performance of numerical tasks at the macroscopic level using the microscopic (e.g., stochastic) simulation codes is the so-called *coarse time-stepper*. It consists of three parts: lifting (mapping from coarse-macroscopic to microscopic level), short time micro calculations around which the macroscopic calculations are wrapped and restriction (mapping from fine-micro scale to macroscopic level) [1]. The details about each part are presented in many papers [1–10]. The coarse time stepper is combined with time projection at macroscopic level, i.e., time projection of the coarse observables on the macroscopic scale. Significant premise in the EFREE framework is the clear separation between micro and macro time scales.

The complexity of plasma phenomena challenged researchers to try to implement the multiscale approaches developed in other scientific fields. One of these attempts is the implementation of the EFREE procedure by Shay et al. [11], in the context of the nonlinear ion-acoustic wave as the preparatory step for the intriguing task to solve a problem of the magnetic reconnection. There, the ion-acoustic wave propagation and steepening are originally followed by the modified three-dimensional electromagnetic particle-in-cell (3D EM PIC) code. In EFREE the electrons are adiabatic, both the electron and ion velocity distributions are assumed to be the shifted Maxwellian and quasineutrality is proposed. The results of the multiscale EFREE calculations are discussed with respect to the full micro-PIC simulations. At the first step the coarse observables are determined. First three moments: ion density, ion velocity and pressure are taken as the 'active' coarse observables, i.e., those macro variables which are directly computed forward in time. On the other hand, the electron density, electron velocity and electric field are taken as the 'passive' coarse variables, i.e., variables which are not calculated directly but from active macro observables. These observables are defined on the coarse mesh by the linear interpolation procedure [11]. The micro quantities, the ion and electron positions are obtained through the *lifting* from corresponding densities and the ion and electron velocities are lifted from corresponding velocity distributions (approximated by the shifted Maxwellian). The PIC solver is then applied for the short time in order to ensure the system to stay near the so-called slow manifold. In other words, the implementation of the micro solver has to ensure the reconstruction of the values of the macro quantities which would be obtained under the same conditions but using only the micro solver. The

coarse-macro observables are generated by the reverse operation-*restriction*. After the linear interpolation they are projected in time. Approximately time interval for the micro calculation is around 20 micro time steps and the macro (projection) time step is two order of magnitude larger than the micro time step [11]. This procedure basically neglects kinetic effects in a plasma. The problems which appeared in the reconstruction of the ion-acoustic wave when the wave steepening is noticed were related to the particle trapping, non-Maxwellian features and violated quasineutrality. Thus, instead of moments, the wavelet technique for reconstructing the particle probability distribution function (PDF) was indicated as a possible solution [11]. The aim of this paper is to further test applicability of the EFREE framework, attempting to include kinetic effects through particle correlations in the nonlinear ion-acoustic wave (IAW) paradigm. This approach uses the marginal and conditional cumulative distribution functions as the macro (coarse) scale observables [10]. The results of the EFREE simulations are compared with the results obtained by the one-dimensional electrostatic particle-in-cell (1D ES PIC) solver [12]. In addition results are compared with the results in [11] and multiscale calculations in the framework of the systems of coupled oscillators [13–16].

2 The ion-acoustic wave

The theoretical modeling of the ion-acoustic waves usually starts with the fluid equations in a form [11]:

$$\begin{aligned}
 \frac{\partial n_i}{\partial t} + \nabla \cdot (n_i \vec{V}_i) &= 0, \\
 m_i \left(\frac{\partial}{\partial t} + \vec{V}_i \cdot \nabla \right) \vec{V}_i &= -\frac{\nabla P_i}{n_i} + e\vec{E}, \\
 0 &= -\frac{\partial P_e}{n_i} - e\vec{E}, \\
 \frac{\partial P_i}{\partial t} + \vec{V}_i \cdot \nabla P_i + \gamma_i P_i \nabla \cdot \vec{V}_i &= 0, \\
 \nabla \cdot \vec{E} &= 4\pi e(n_i - n_e),
 \end{aligned} \tag{2.1}$$

where n is density, \vec{V} is velocity, P is pressure, and the subscript ' i ' and ' e ' refers to positive ions (protons) and electrons, respectively. In equations (2.1) the electron inertia term (m_e) is ignored and because the electron thermal velocity is so much larger than the ion-sound speed, the isothermal electrons ($\gamma_e = 1$) are used. Initially the electron temperature is constant in space, which allows to keep relation $\nabla P_e = T_e \nabla n_e$ for all time. The dispersion relation for ion-acoustic waves:

$$\begin{aligned}
 \omega^2 &= \frac{k^2 C_{se}^2}{1 + k^2 \lambda_{de}^2} + k^2 C_{si'}^2, \\
 C_{se}^2 &= \frac{T_e}{m_i}, \quad C_{si'}^2 = \frac{\gamma_i T_i}{m_i}, \quad \lambda_{de} = \frac{C_{se}}{\omega_{pi}},
 \end{aligned} \tag{2.2}$$

can be obtained by the linearization of (2.1) by introducing a small perturbation in a form:

$$f(\vec{x}, t) = f_0(\vec{x}) + \tilde{f} e^{i(\vec{k} \cdot \vec{x} - \omega t)}, \quad (2.3)$$

for the electron and ion densities ($f = n_i, n_e$), assuming the vanishing initial velocities, the weak ion Landau damping and the non-isothermal condition, $T_e/T_i \gg 1$ [11].

2.1 One-dimensional electrostatic Particle-in-Cell code

We have employed a one-dimensional electrostatic Particle-in-Cell (PIC) code based on es1 [12]. The ion and electron ensembles are initialized in the position - velocity space by the quiet start procedure [12] assuming the Maxwellian velocity distribution for both species.

The value of the particle charge densities are sampled by the first order weighting smoothness or the cloud-in-cell (CIC) procedure [12]. This procedure significantly reduces noise in the system. The new mesh is built of nx grids (in x direction). The charge density is used for determination of the electrostatic field on the corresponding mesh through the Poisson equation:

$$\begin{aligned} E &= -\frac{\partial \phi}{\partial x}, \\ \frac{\partial^2 \phi}{\partial x^2} &= -\frac{\rho}{\epsilon_0}, \end{aligned} \quad (2.4)$$

where ρ is the charge density and E is the electric field. In numerical calculations the Poisson equation is solved by the fast Fourier transform [12]. The field values at particle positions are determined by the interpolation procedure.

The particle equations ($i = N$ equations) of motion:

$$\begin{aligned} m \frac{dv_i}{dt} &= F_i = q_i E, \\ \frac{dx_i}{dt} &= v_i, \end{aligned} \quad (2.5)$$

are replaced by the finite-difference equations and solved by the leap-frog method [12]. All quantities are normalized to the ion scale: the ion plasma frequency, the ion Debye length, and the IAW period, respectively.

The set of parameters (normalized) in this paper is: $L = 1.2$, $dt = 0.0001$, $N_e = N_i = N = 252144$, $w_{pe} = 5091$, $q_e/m_e = -1.0$, $v_{te} = 42.5$, $w_{pi} = 120$, $q_i/m_i = 0.00056$, $v_{ti} = 0.22$, $nx = 512$, the particle drift velocities are initially taken as zero. Note that above corresponds to the similar parameter set as in [11].

The macro (coarse) observables are the total energy and the particle densities. Their values obtained by the 1D ES PIC code and EFREE procedure are compared and used to estimate the possible benefits of the EFREE approach.

3 Equation-free coarse projective integration

To resolve a multiscale phenomenon and propagate its influence across scales is the crucial goal of mathematical and physics based models. If no explicit coarse-grained, macroscopic equations are available, the EFREE framework has been proposed [1–4]. Equation-free methods numerically evolve the coarse-scale behavior through appropriately designed short computational experiments performed by the fine scale (microscopic) models. One of the EFREE methods is coarse (macro) projective integration. The macro projective integrator consists of a coarse scale time-stepper and projection step in time, or the temporal evolution of the macro observables [1–4].

3.1 A coarse time-stepper

The coarse time-stepper is the basic element for exchanging information between coarse-scale model states and fine-scale states. It consists of three parts: *lifting*, *micro-scale evolution* and *restriction*. The lifting transforms coarse-scale macro observables to consistent fine-scale states; restriction is the reverse transformation, from fine-scale states to coarse-grained observable. These two transformations applied successively should give the identity on the coarse observables up to modulo round-off error [1–4].

In the standard approach for many multiscale problems observed along a single effective spatial dimension, the particle positions constitute the fine-scale model state and the local mean particle concentration constitutes the coarse-grained state. Then the local mean concentration is observed in terms of a histogram of the single particle position probability distribution function (PDF). However, the PDF histogram depends on a bin size used for estimation. Moreover, the PDF may become zero if the bin size is too small so that no particle is inside it [1, 17]. To overcome these difficulties the cumulative distribution function (CDF) is used as an alternative coarse-scale observable. Actually, the inverse CDF (ICDF) which is supported in $[0,1]$ is constructed instead the CDF which has in principle infinite support. The ICDF is further estimated by its projection on some chosen orthogonal polynomial set [9, 10].

The fundamental problem in multidimensional particle systems originates from an infeasibility to define the multidimensional CDF. Therefore, the idea is to substitute the multidimensional CDF (ICDF) by defining the set of one-dimensional CDF-s (ICDF-s) [10]. For two dimensional case, which is here of interest, the 2D CDF can be represented in a form:

$$F_{XV}(x,v) = \int_{-\infty}^v F_{X|V}(x|v) \frac{dF_V(v)}{dv} dv, \quad (3.1)$$

where $F_{XV}(x,v)$, $F_V(v)$ and $F_{X|V}(x|v)$ are the 2D CDF, differentiable marginal CDF (MCDF) and conditional CDF-s (CCDF), respectively. The CCDF is defined by the probability of the particle positions to have values up to some fixed x while the corresponding particle velocities are in infinitesimally small interval $(v, v + \Delta)$, or in the language of the

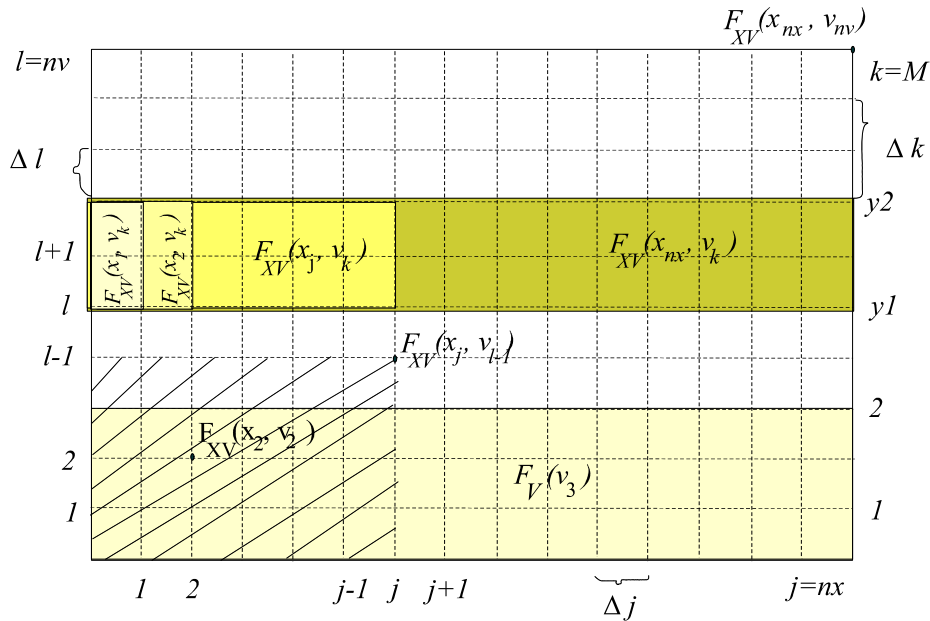


Figure 1: 2D 'phase-space' and the cumulative distribution functions: 2D CDF, MCDF and CCDF-s.

CDF-s:

$$F_{X|V}(x|v) = \lim_{\Delta v \rightarrow 0} \frac{F_{XV}(x, v + \Delta v) - F_{XV}(x, v)}{F_V(v + \Delta v) - F_V(v)}. \quad (3.2)$$

Assuming smoothness, a finite number of the CCDF-s can be used to recover (for example through interpolation) the particle distribution. Schematic presentation of the CDF-s is given in Fig. 1.

3.1.1 Lifting

The lifting procedure starts with the ICDF-s for the marginal and several 1D conditional distributions. The number of latter ones is determined by the smoothness of the 2D phase space. In practice, the velocity of the i^{th} particle is directly taken from the marginal ICDF as $v_i^s = IF_V((i - 0.5)/N)$, $i = 1, 2, \dots, N$, where N is the total number of particles and superscript s indicates that v_i^s are sorted in monotonically ascending sequence which reminds on the so called *quiet start* procedure. Then corresponding to each v_i^s is the particle position x_i determined as $x_i = IF_{X|V}(U_i, v_i^s)$, where U_i are uniformly distributed real random values over $[0, 1]$. Actually, as was noted, only a few conditional CDF-s are needed if the particle distribution over phase space is sufficiently smooth [9]. Therefore, for each particular v_i^s the CCDF-s available in its neighborhood (e.g., the closest one, or an interpolation of the closest ones) are employed.

Let the number of CCDF-s be M ($M \ll N$). Then the inverse CCDF is given by $IF_{X|V}(f, v_k^s)$, $k = 1, 2, \dots, M$, where f is from $[0, 1]$, and $v_k^s = v_{(k-1)int(N/M) + int(N/2M)}^s$. There-

fore, the particles are lifted to their positions with respect to the v_k^c , i.e., $x_{ik} = IF_{X|V}(U_{ik}, v_k^c)$, where $ik = 1, 2, \dots, n_k$, n_k is the number of particles in k^{th} layer in v -space and $n_1 + n_2 \dots + n_M = N$. By this procedure the particle correlations are implicitly better preserved than in the EFREE procedures which are based on the PDF-s or 1D CDF-s.

3.1.2 Fine-scale evolution

In the ion-acoustic wave problem, the ensembles of the $N_e = N$ electrons and $N_i = N$ ions are followed in the self-consistent electrostatic field. The fine-scale model state consists of the electron and ion positions and velocities, i.e., the model state is represented by a point in the corresponding $2N$ D phase space, (x_i, v_i) , $i = 1, 2, \dots, N$. The micro-scale particle dynamics is modeled by the 1D ES PIC numerical routine [12] and corresponding fine-scale (micro-scale) state is visualized in the $2D$ (x, v) space for each of mentioned species. Being basically the collective phenomenon, the plasma ion-acoustic wave involves the correlations in particle motion which are observed through the periodic pattern in the numerical PIC experiment [11, 18], as can be seen in Figs. 3-6 g,h. The wave pattern formation is interpreted as a consequence of the space-time particle position and velocity correlations in the (x, v) phase space. Therefore, the above described procedure based on the conditional cumulative distributions is adopted. In addition the separation of the ion- and electron- correlation time is assumed which is the necessary assumption for the implementation of the multi-scale procedure [1, 2, 11]. In other words, the application of EFREE CCDF procedure assumes: the ion correlation time (ion plasma period) \gg the electron correlation time (electron plasma period).

Nonlinear evolution of the ion-acoustic wave involves in the latter phase ($t \sim 0.5$) the ion trapping effects, Figs. 5-6. The new characteristic (correlation) time is the bounce time which is between the electron and ion PIC correlation time. Therefore, if it is not possible to clearly separate the correlation timescales, the application of the EFREE maybe under question. This point will be discussed in the next section.

3.1.3 Restriction

The mapping from fine-scale to coarse-scale state is started by sorting the particle velocities $\{v_i^s\}$, $i = 1, 2, \dots, N$, in the ascending order. To preserve the correlations the corresponding particle positions are sorted as $\{x_i^s\}$.

Then $2D$ mesh is formed with each grid point having a coordinate (x_j^s, v_l^s) , $j = 1, 2, \dots, nx$, $l = 1, 2, \dots, nv$, ($nx, nv \ll N$). For each (x_j^s, v_l^s) grid point, the number, N_f , of particles which x and v coordinates satisfy $x_i \leq x_j^s$ and $v_i \leq v_l^s$, respectively, is counted and the CDF at this grid point evaluated as

$$F_{XV}(x_j^s, v_l^s) = \frac{N_f - 0.5}{N}. \quad (3.3)$$

This is only one of several possibly applicable restriction methods [8,9,17]. Assuming the

CDF to be differentiable, that the CCDF (7) can be written in a form:

$$F_{X|V}(x_j^s|v_k^s) = \frac{F_{XV}(x_j^s, v_{y2}^s) - F_{XV}(x_j^s, v_{y1}^s)}{F_{XV}(x_{nx}^s, v_{y2}^s) - F_{XV}(x_{nx}^s, v_{y1}^s)}, \quad (3.4)$$

where $k=1, \dots, M$ ($M \leq nv \ll N$), and $y1$ and $y2$ can be chosen as $(k-1)int(nv/M)+1$ and $kint(nv/M)$, respectively. Once the CCDF is available numerically, the conditional ICDF $IF_{X|V}(f, v_k^s)$ can be evaluated as one-dimensional inverse cumulative distribution by the standard subroutine in the PIC code [12].

3.2 Projection step in time

The projection step in time, or the temporal evolution of the coarse observables, is realized by the least-square method [2, 11] briefly described in the following. The value of each coarse observable is collected from the successive mf time steps (the micro-time steps, dt , or several micro-time steps long) including the projection time t_p . With these mf values the fitting procedure based on the least-square technique is initialized and the value of coarse observable at the coarse-time scale, $t=t_p+\Delta t$, is estimated, where $\Delta t \gg dt$. The separation of the electron and ion correlation time determines the relation between the micro and macro time step. In addition, the Courant condition [12] should be kept in mind. Generally, the macro time step, Δt , is defined on the ion scale and micro time step, dt , on the electron time scale: $\Delta t \sim 10-50dt$. Problem appears when the ion trapping becomes pronounced, because the clear separation among the time scales disappears.

We note that the polynomial fitting procedure was also tested. After comparing the results from different fitting schemes finally the least-square fitting was chosen.

4 Results and discussion

The presentation in Section 3 of the coarse time-stepper routine for the ion-acoustic wave was of a general type. Thus, in the following, concrete realization is briefly illustrated.

At first, the set of coarse observables is identified to which the fine-scale model states for the ion and electron species are restricted. The set of coarse ion observables consists of the proper number of the expansion coefficients in the Lagrange polynomial basis [9] of the MCDF, $F_V(v)$, and the several CCDF-s ($F_{X|V}^k(x|v), k=1, 2, \dots, M$). Number of the significant expansion coefficients and the number of the CCDF-s are determined by the direct numerical estimations. Here presented results are generated over the 2D mesh which consists of $(nx, nv) = (512, 1e^5)$ grid points, the number of expansion coefficients is 30 and $M=100$ (the values of other parameters are written in Section 2). The former value is closely related to the smoothness of the corresponding MCDF and the latter to the smoothness of the CCDF-s (Fig. 2).

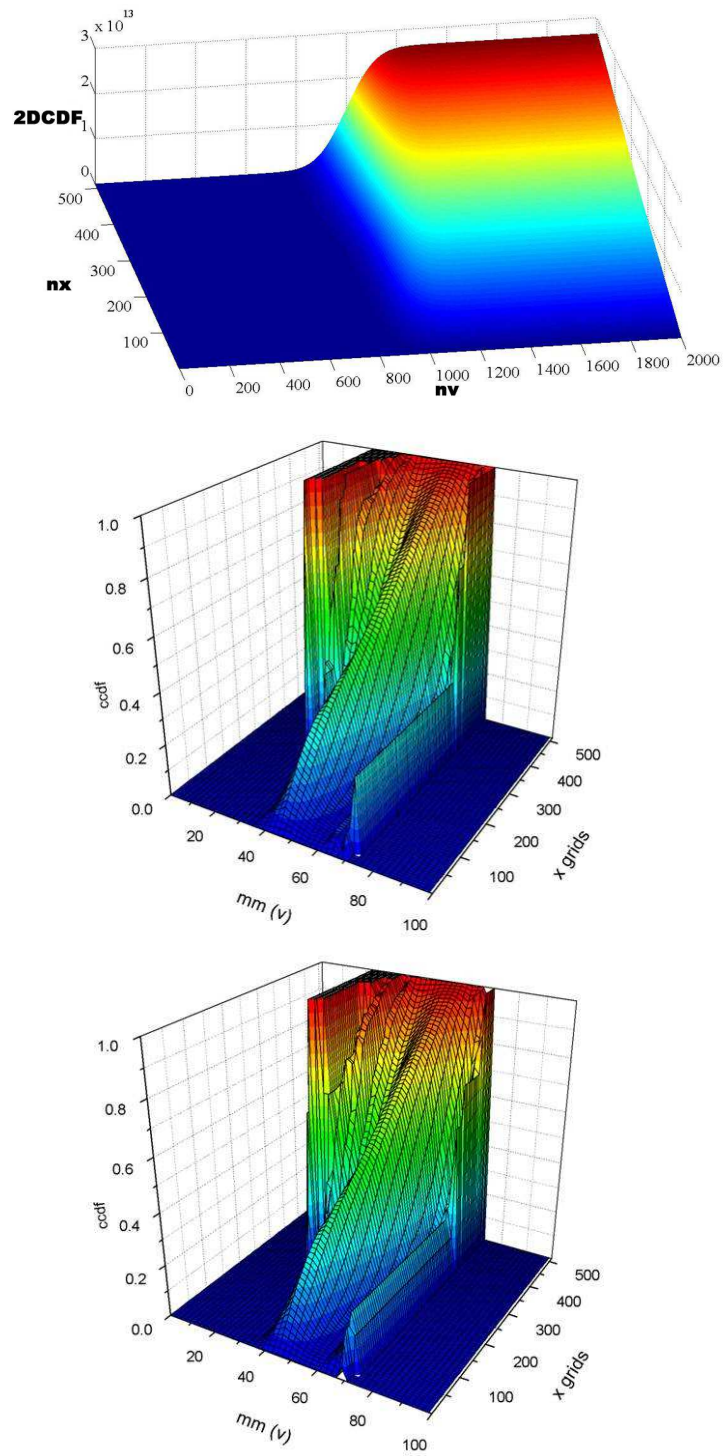


Figure 2: The ion 2D CDF, CCDF at $t=t_p=0.1$ and CCDF after applying lifting and restriction. The parameter set is given in Section 2.

The set of the coarse electron observables consists of the marginal CDF, $F_V(v)$, and density distribution which is determined from the corresponding ion charge density distribution assuming the adiabaticity [11].

The ion positions and velocities can be lifted from the corresponding coarse observables through the lifting procedure described in Section 3.1.1. The electron velocities are lifted from the electron MCDF by the same procedure as ion velocities are lifted from the corresponding ion MCDF. On the other hand, electron positions are lifted from the electron charge density which is then interpreted as the MCDF in the coarse grid in x space.

The noise is inherently present in each particle simulation [12] due to a finite number of particles per grid. However, the additional noise appears during the restriction-lifting procedure. In order to decrease it, the linear interpolation scheme introduced in [11] is adopted to the ion charge distribution. The linear interpolation is realized in the following way. The restricted, coarse observable-ion charge density after the first interpolation level is:

$$\rho_i^{(1)} = 0.25\rho_{2i-1} + 0.5\rho_{2i} + 0.25\rho_{2i+1}, \quad i = 1, \dots, n_m/2, \quad (4.1)$$

where $nm = 512$. Note that the periodic boundary conditions are assumed. The $\rho^{(l)}$ value is defined at $2^{-l}nm = nc = 32$ grid points after l levels of interpolation. The ρ over the coarse mesh with nc grids is then projected in time. Before lifting the number of mesh grids is expanded to the nm grids. In other words, the linear interpolation is once more called. Supposing the nc coarse data points for the variable ρ , the first level of interpolation is:

$$\rho_{2i}^{(1)} = \rho_i, \quad \rho_{2i-1}^{(1)} = 0.5(\rho_{i-1} + \rho_i), \quad i = 1, \dots, n_c. \quad (4.2)$$

Periodic boundary conditions are assumed. After l iterations, $\rho^{(l)}$ will be defined at mesh with $nm = 2^l nc = 512$ grid points. Therefore, the ion charge distribution collected in nm positions, i.e., the corresponding electron density is the coarse observable for a lifting step. The interpolation was also shown as necessary in order to be consistent with the Courant condition [11, 12]. Somewhat unexpected, although the explicit Courant condition has not figured in the ES particle code, in the EFREE macro projection phase, this condition emerges as the stability criterion [11, 18]. Roughly, the macro time step (projective time step) has to be consistently chosen with respect to the finite speed of the information transfer between the neighboring mesh grids in the simulation procedure. The characteristic speed is the ion sound speed [11]. Thus, a larger macro time step requires a bigger mesh cell. In practice this could be realized by time projection of the coarse grained restricted quantities defined on the new mesh with smaller number of grids. It is one reason more to project in time the density on the $nc = 32$ spatial grids instead on the 512 grids. However, the projection time step (macro time step) appeared limited to the $10 - 20dt$ (micro time steps). Likely, not clear separation between the nonlinear IAW and electron time scales is the one of possible reasons.

The lifting phase is followed by the fine-scale evolution which is realized by the 1D ES PIC micro solver [12]. A crucial point is to determine an optimal time duration for short

bursts of micro simulations in order to ensure that the system relaxes and always stays near the slow-manifold; and to recover best possible values of macro (coarse) observables closest to those that would be obtained by a direct micro solver (PIC simulations). Fact that the regular ion-acoustic periodic wave pattern exists only in the limited time interval to $t \sim 0.5 = 5000dt$ shows the main difficulty to determine the optimal interval for micro bursts. The discussed points are illustrated in Figs. 3-6, which present the best results after a large number of the numerical checks.

In Figs. 3-6 the snapshots of the ion density (a), electron density (b), marginal velocity PDF for electrons (c) and ions (d), and the corresponding phase spaces obtained by the full PIC and EFREE procedure are presented. Black curves in (a)-(d) are generated by the PIC code and the red ones by the EFREE procedure. In addition, Fig. 7 illustrates time development of the electron and ion kinetic energy, electric field energy and total energy for parameter set in Section 2. The dark curves represent the EFREE and light curves the results of full PIC calculations. In addition, in Fig. 8 the results of PIC simulations and the EFREE projective integration are compared by defining the relative error [12]:

$$\varepsilon^2 = \frac{\sum_{j=1}^{n_{xc}} (f_j^{efree} - f_j^{pic})^2}{\sum_{j=1}^{n_{xc}} ((f_j^{efree})^2 - (f_j^{pic})^2)^2}, \quad (4.3)$$

where f_j EFREE and PIC are the value of the coarse observable in the EFREE and PIC output, respectively. In Fig. 8, errors for the electron and ion density are plotted. The maximal value of the square root of the relative error is around 5%. Results presented correspond to projective time step equal to 10 micro steps. During macro projective procedure the time stepper parts are checked separately, as mentioned in our several earlier contributions [18].

The macro quantities, the ion and total energy obtained by the full PIC calculations are nicely reproduced by the multiscale procedure in a time interval up to $t < 0.5$, where the separation of the ion and electron time scale is visible. However, clear separation of time scales is absent when ion trapping is initialized as can be seen in the ion phase space. This moment can be interpreted as a critical or bifurcation point as clearly manifested through the relative errors plots in Fig. 8. Therefore, in this study, the application of the projective integration routine becomes questionable after $t \sim 0.5$.

Let us return to the results in Figs. 3-6 to summarize several crucial points. The noise is accumulated gradually with respect to the case with full PIC, as seen in Figs. 3-6. This problem can be associated with the non-smoothness in the boundary layers in v -space of the corresponding CCDF (Fig. 2). On the other hand, this is a reflection of poor statistics (small number of ions) in these regions of phase space after the ion-wave (periodic) structures are developed. In addition, any implementation of the lifting step induces some percentage of noise. Trying to overcome the noise problem by additional interpolation of the coarse quantities before lifting has not given much improvement.

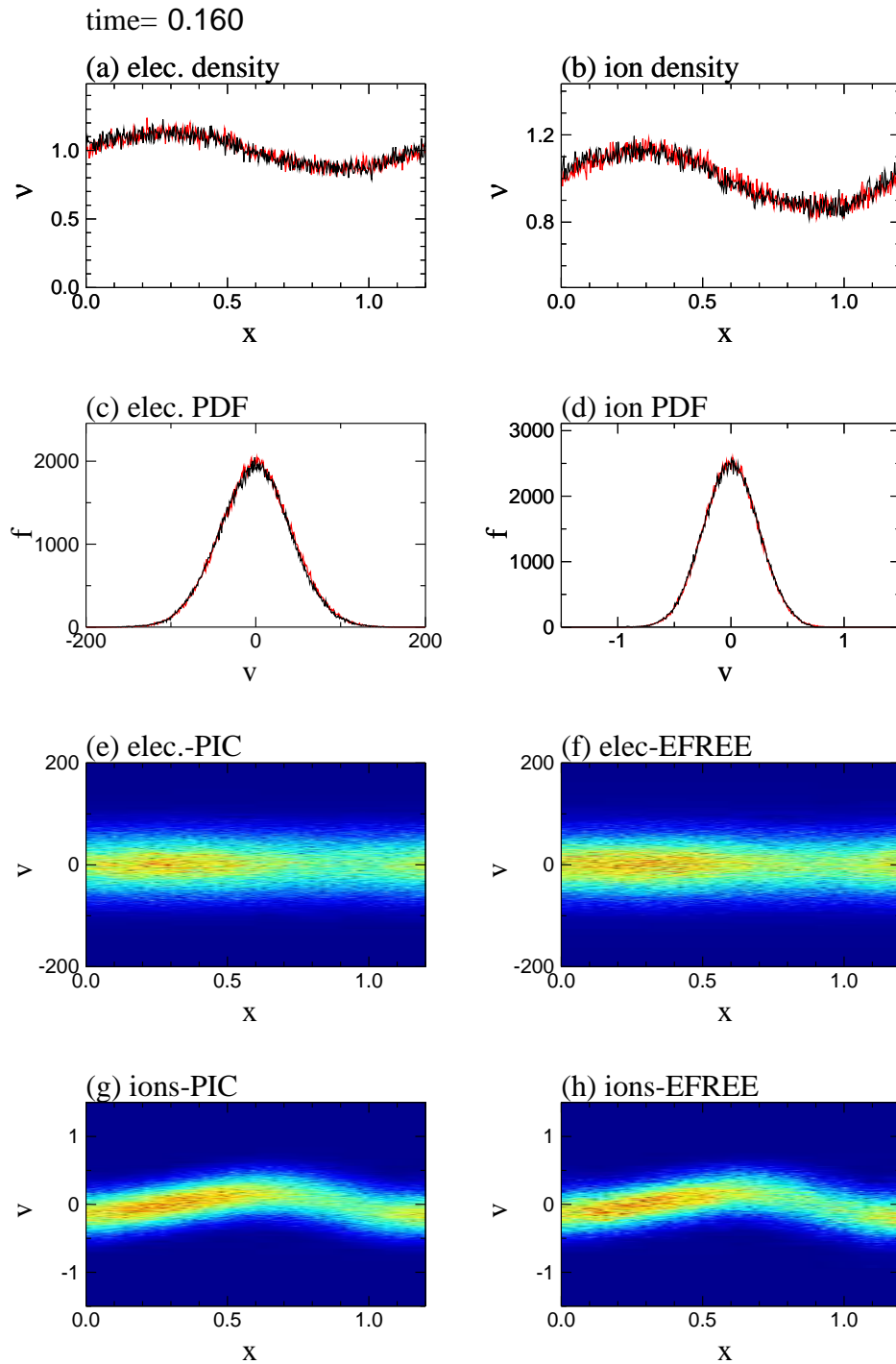
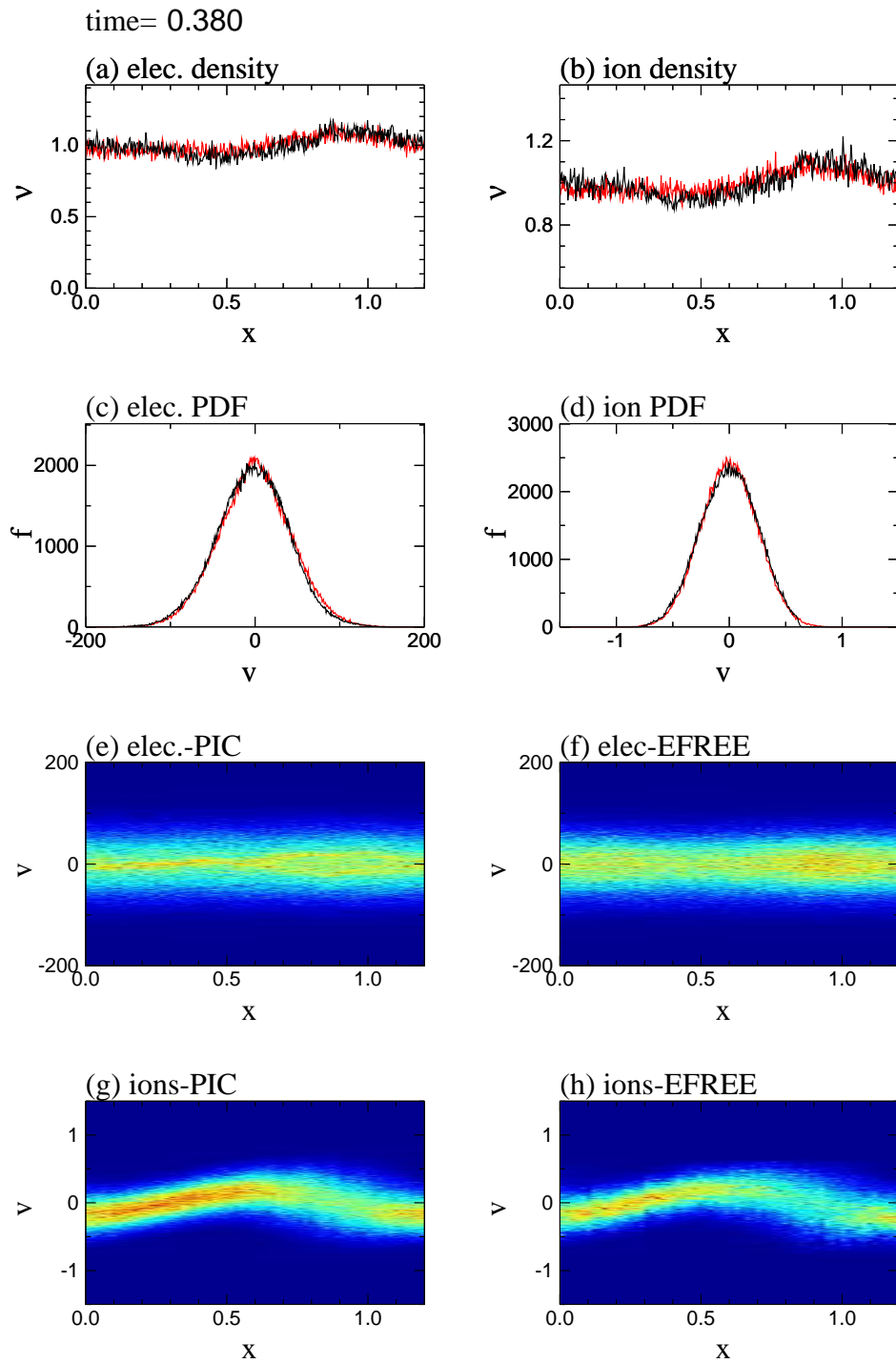


Figure 3: Snapshots of the ion density (a), electron density (b), marginal velocity PDF for electrons (c) and ions (d), and the corresponding phase spaces obtained by the PIC code and EFREET procedure at $t=0.16$. Black curves in (a)-(d) are generated by the PIC code and the red ones by the EFREET procedure.

Figure 4: Same as Fig. 3, except at $t=0.38$.

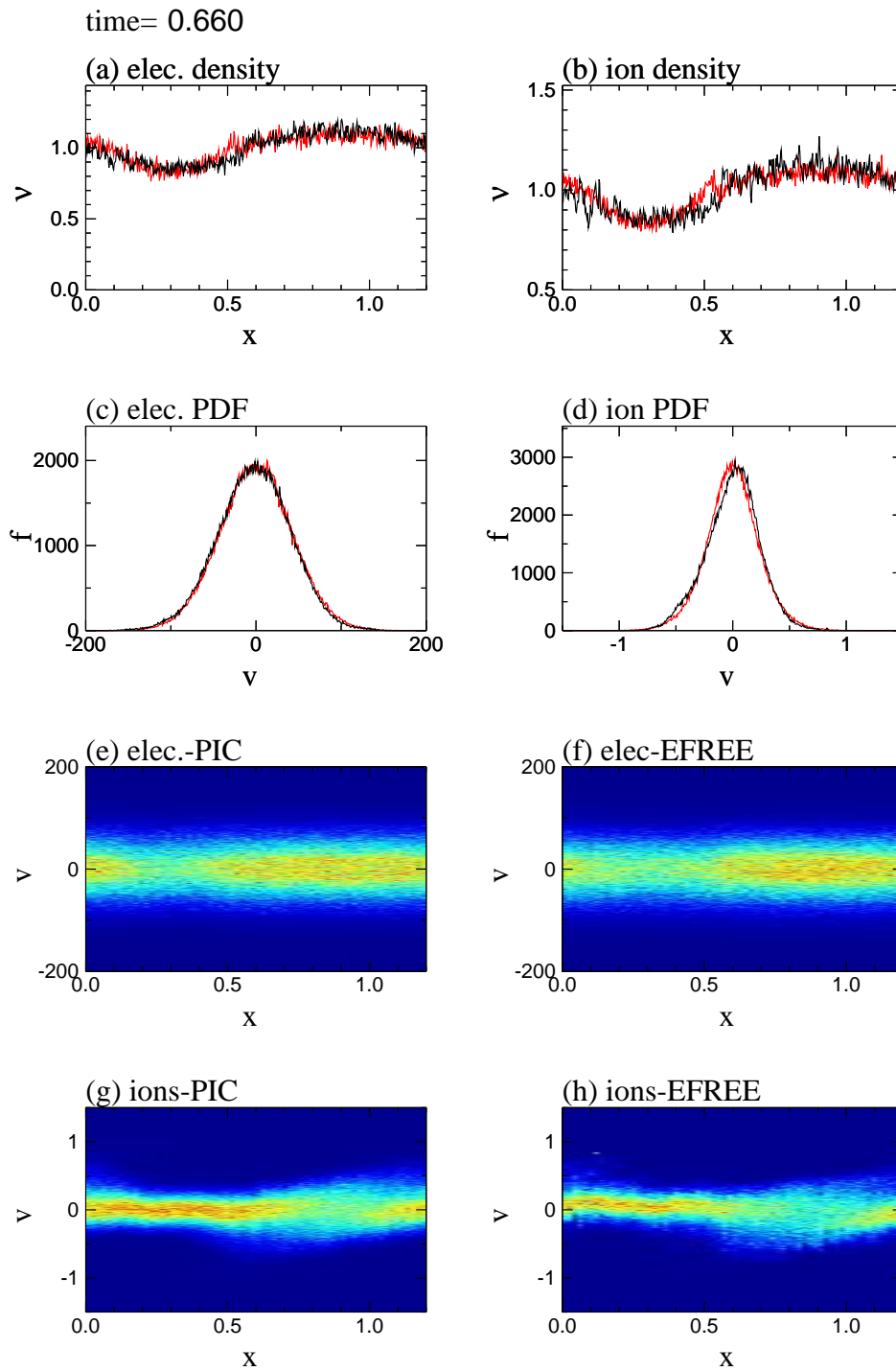
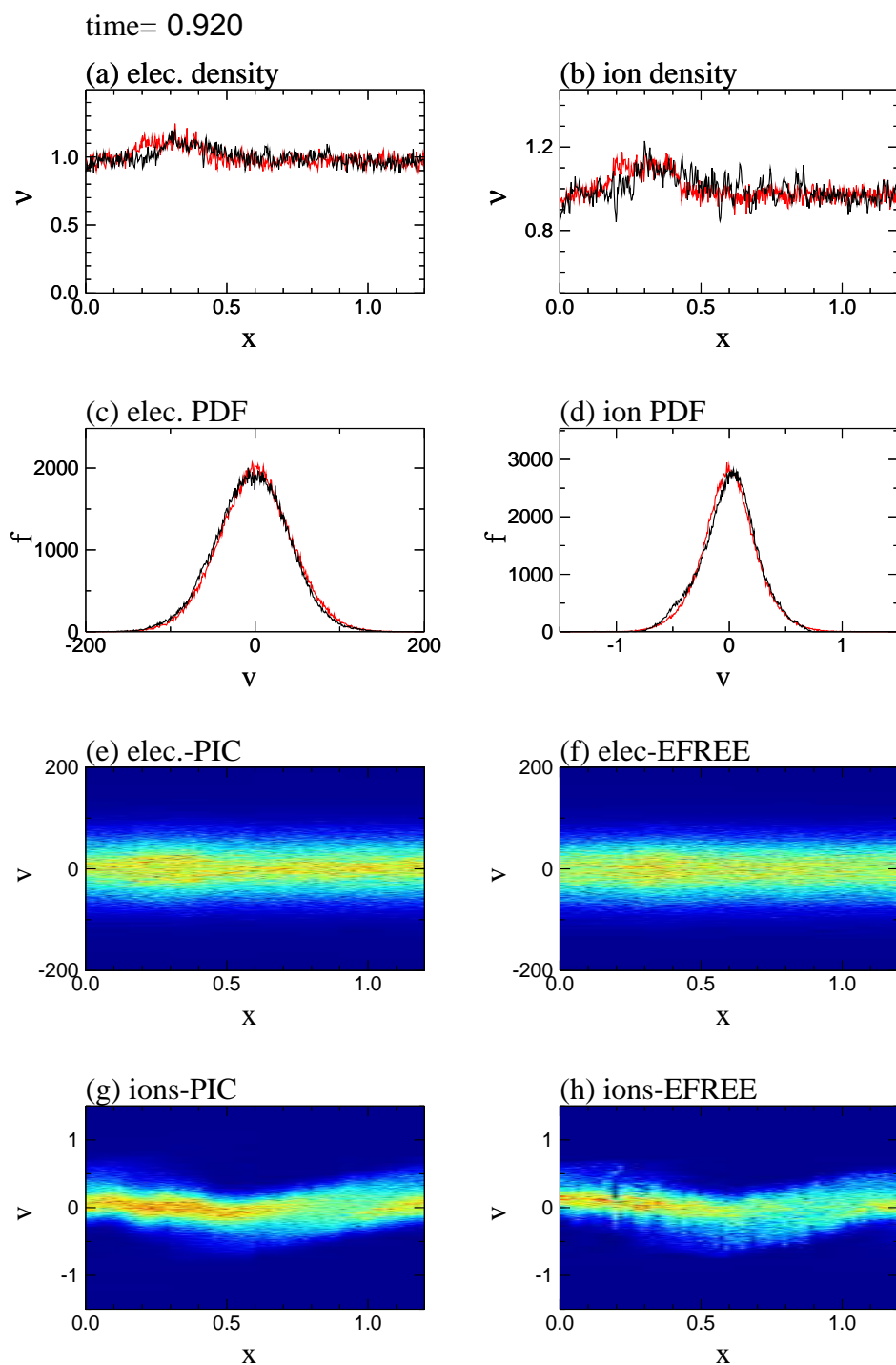


Figure 5: Same as Fig. 3, except at $t=0.66$.

Figure 6: Same as Fig. 3, except at $t=0.92$.

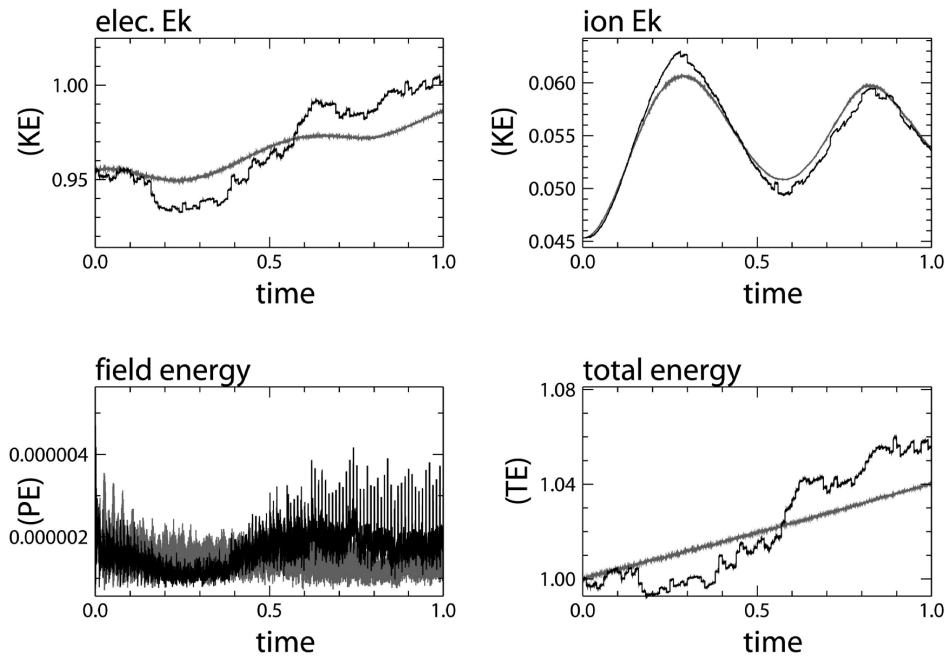


Figure 7: The particle kinetic energies, electric field energy and total energy by PIC (grey) and EFREE.

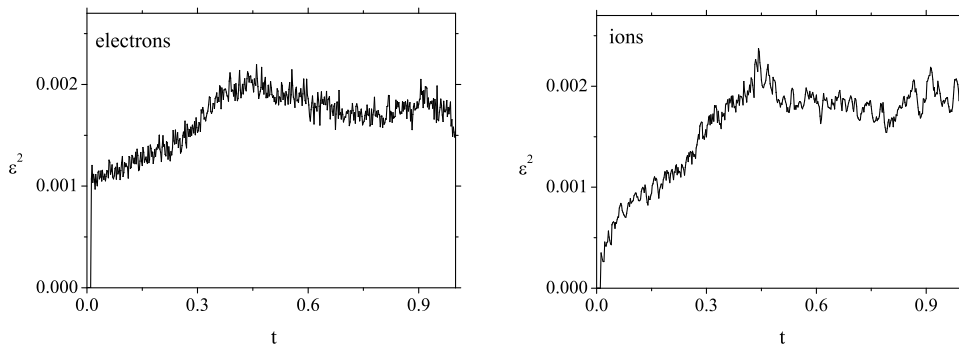


Figure 8: Relative error estimated by Eq. (4.3) for electrons and ions.

The lifting operation is not uniquely defined. In other words, naturally many different micro configurations correspond to the one macro state. This problem is partially eliminated if the aim is to interpret evolution of the random, uncorrelated systems far away from the critical points. There the probability of the most micro configurations is equal. Only in such a steady case the clear separation of the micro and macro scale is obvious. This is opposite to the ion-acoustic case treated here, where the collective phenomena gradually build coherent structures increasing the correlation rate in a system. That the lifting is critical step for the coherent-periodic (collective) processes is already indicated in references [13–16] which are the pioneering attempts to implement the multiscale considerations in the coupled oscillator's framework.

At this point it is worth to overview our results with respect to some other works on the EFREE framework. The similar problems mentioned here appeared in the EFREE treatment by Shay et al. [11], which, actually, gave the motive to start this work. At first sight their results might look better by comparing the relative errors after implementation of the EFREE procedure and used projective time step. However, by a closer inspection, these results are not fully clarified because the energy conservation has not been presented. There are several uncertain points which influence to guess that the energy conservation condition might be already violated in the very early stage of the projective integration. It is especially expected with respect to the used large projective time step and consistency with the Courant condition. In addition, our experience after many numerical calculations also indicates that the wavelet expansion, which is mentioned in [11, 19], may not be sufficient to overcome the noise and particle correlation problems. Finally, although the qualitative presentation of the projective integration based on the conditional cumulative technique is of our concern, it is worth mentioning that the improved numerical procedures could possibly eliminate the part of a problem which appeared here.

5 Conclusion

This work is one of the first attempts to test a method in the EFREE framework on the plasma physics phenomenon. A new macro projective integration scheme developed for two-dimensional microscopic systems was applied to the plasma ion acoustic wave. The method consists of two parts: time stepper (lifting, micro simulation, restriction) and time projection over the macro time scale. Time stepper is based on the one-dimensional cumulative distribution functions as the coarse observables. These are the marginal cumulative and several conditional cumulative distribution functions. The concrete number of the coarse observables depends on the smoothness of the particle distributions, related to the correlation among particles due to appearance of coherent wave structures. The micro solver for the ion acoustic wave is the one-dimensional ES PIC code.

Our calculations indicate that the unclear separation of the micro and macro physics scales in the nonlinear ion acoustic wave evolution is a crucial difficulty for working in the EFREE framework. In addition, noise level which is inherent in PIC simulations has been increasing specially during the repeating lifting phase in the procedure. Therefore, it seems that the ion acoustic paradigm with the PIC micro solver may not be an adequate test for the EFREE framework. Still, this should not discourage researchers to consider alternative multiscale plasma physics problems in the EFREE context.

Acknowledgments

This work is performed with the support under the auspices of the NINS-NIFS Collaborative Project (NIFS05KEIN0041, NIFS06KEIN0041) and NIFS Collaborative Research

Program (NIFS04KDAT007, NIFS05KDAT007, NIFS07KDAN001). One of us (A.M.) acknowledges partial support by the Ministry of Science and Protection of Environment of Serbia, Project 141034.

References

- [1] I. G. Kevrekidis, C. W. Gear, J. M. Hyman, P. G. Kevrekidis, O. Runborg and C. Theodoropoulos, Equation-free, coarse-grained multiscale computation: Enabling microscopic simulators to perform system-level analysis, *Comm. Math. Sci.*, 1 (2003), 718-782.
- [2] R. Erban, I. G. Kevrekidis and H. G. Othmer, An equation-free computational approach for extracting population-level behavior from individual-based models of biological dispersal, *Physica D*, 215 (2005), 1-24.
- [3] A. G. Makeev, D. Maroudas, A. Z. Panagiotopoulos and I. G. Kevrekidis, Coarse bifurcation analysis of kinetic Monte Carlo simulations: A lattice-gas model with lateral interactions, *J. Chem. Phys.*, 117 (2002), 8229-8240.
- [4] O. Runborg, C. Theodoropoulos and I. G. Kevrekidis, Effective bifurcation analysis: A time-stepper-based approach, *Nonlinearity*, 15 (2002), 491-511.
- [5] R. Rico-Mertinez, C. W. Gear and I. G. Kevrekidis, Coarse projective kMC integration: Forward/reverse initial and boundary value problems, *J. Comput. Phys.*, 196 (2004), 474-489.
- [6] C. W. Gear, T. J. Kaper, I. G. Kevrekidis and A. Zagaria, Projecting to a slow manifold: Singularly perturbed systems and legacy codes, *arxiv:physics/0405074 v1* (2004).
- [7] D. Liu and I. G. Kevrekidis, Equation-free multiscale computation for unsteady random diffusion, *SIAM Multiscale Model. Simulat.*, 4 (2005), 915-935.
- [8] S. Setayeshgar, C. W. Gear and I. G. Kevrekidis, Application of coarse integration to bacterial chemotaxis, *Multiscale Model Simulations*, 4 (2005), 307-327.
- [9] C. W. Gear, Projective integration methods for distributions, *NEC Transactions*, p.130 (2001).
- [10] Y. Zou, I. G. Kevrekidis and R. G. Ghanem, Equation-free particle-based computations: Coarse projective integration and coarse dynamic renormalization in 2D, *Ind. Eng. Chem. Res.*, 45 (2006), 7002-1014.
- [11] M. A. Shay, J. F. Drake and B. Dorland, Equation free projective integration: A multiscale method applied to a plasma ion acoustic wave, *J. Comput. Phys.*, 226 (2007), 571-585.
- [12] C. K. Birdsall and A. B. Langdon, *Plasma Physics via Computer Simulation*, Adam Hilger, Bristol, Philadelphia and New York, 1991.
- [13] P. Van Leemput and W. Vanroose, Initialization of a lattice Boltzmann model with constrained runs (Extended Version), Katholieke Universiteit Leuven, Report TW 444 (2005).
- [14] K. A. Bold, Y. Zou and I. G. Kevrekidis, Heterogeneous cell population dynamics: Equation-free uncertainty quantification computations, *arxiv:q-bio.QM/0611001 v1* (2006) (submitted to *Biophysical Journal*).
- [15] G. Samaey, W. Vanroose, D. Roose and I. G. Kevrekidis, Coarse-grained computation of traveling waves of lattice Boltzmann models with Newton-Krylov solvers, *arxiv:physics/0604147 v1* (2006).
- [16] S. J. Moon, R. Ghanem and I. G. Kevrekidis, Coarse-graining the dynamics of coupled oscillators, *Phys. Rev. Lett.*, 96 (2006), 144101.
- [17] J. Li, P. G. Kevrekidis, C. W. Gear and I. G. Kevrekidis, Deciding the nature of the coarse equation through microscopic simulations: the Baby-Bathwater scheme, *SIAM MMS*, 13 (2003), 391.

- [18] M. M. Skoric, S. Ishiguro and S. Maluckov, On a primal coarse projective integration method for multiscale simulations, APS- DPP 48th Annual Meeting, Philadelphia, 2006. <http://meetings.aps.org/Meeting/DPP06/Event/52475>
- [19] G. Stantchev, A. Maluckov, M. Shay, J. Drake, W. Dorland, S. Ishiguro and M. M. Skoric, Wavelet techniques for coarse projective integration in multiscale plasma dynamics, 33rd EPS Conference on Plasma Physics, Rome, 2006.